J Comput Neurosci (2012) 33:77–95
DOI 10.1007/s10827-011-0375-3

Co-variation of ionic conductances supports phase maintenance in stomatogastric neurons

Wafa Soofi · Santiago Archila · Astrid A. Prinz

Received: 15 July 2011 / Revised: 17 November 2011 / Accepted: 21 November 2011 / Published online: 3 December 2011
© Springer Science+Business Media, LLC 2011

Abstract Neuronal networks produce reliable functional output throughout the lifespan of an animal despite ceaseless molecular turnover and a constantly changing environment. Central pattern generators, such as those of the crustacean stomatogastric ganglion (STG), are able to robustly maintain their functionality over a wide range of burst periods. Previous experimental work involving extracellular recordings of the pyloric pattern of the STG has demonstrated that as the burst period varies, the inter-neuronal delays are altered proportionally, resulting in burst phases that are roughly invariant. The question whether spike delays within bursts are also proportional to pyloric period has not been explored in detail. The mechanism by which the pyloric neurons accomplish phase maintenance is currently not obvious. Previous studies suggest that the co-regulation of certain ion channel properties may play a role in governing neuronal activity. Here, we observed in long-term recordings of the pyloric rhythm that spike delays can vary proportionally with burst period, so that spike phase is maintained. We then used a conductance-based model neuron to determine whether co-varying ionic membrane conductances results in neural output that emulates the experimentally observed phenomenon of spike phase maintenance. Next, we utilized a model neuron database to determine whether conductance correlations exist in model neuron populations with highly maintained spike phases. We found that co-varying certain conductances, including the sodium and transient calcium conductance pair, causes the model neuron to maintain a specific spike phase pattern. Results indicate a possible relationship between conductance co-regulation and phase maintenance in STG neurons.

Keywords Stomatogastric system · Pyloric neural network · Model neuron database · Conductance-based model · Phase maintenance

Action Editor: Frances K. Skinner

Electronic supplementary material The online version of this article (doi:10.1007/s10827-011-0375-3) contains supplementary material, which is available to authorized users.

W. Soofi (✉)
Wallace H. Coulter Department of Biomedical Engineering,
Georgia Institute of Technology/Emory University,
313 Ferst Drive,
Atlanta, GA 30332, USA
e-mail: wafa.soofi@gatech.edu

S. Archila · A. A. Prinz
Department of Biology, Emory University,
1510 Clifton Rd NE,
Atlanta, GA 30322, USA

1 Introduction

Neural central pattern generating circuits are able to maintain consistent rhythmic activity throughout the lifetime of the animal. To retain network functionality, each neuron must preserve its unique electrical role within the network. This role is partially governed by each cell's set of membrane currents (Levitan 1988), which must be constantly regulated in order to maintain a consistent electrical identity. This identity is preserved even as the proteins that compose the membrane ion channels undergo turnover (LeMasson et al. 1993). The mechanism by which neurons regulate their membrane currents to maintain network function is, as of yet, not entirely understood.

The pyloric pattern-generating circuit of the stomatogastric nervous system (STNS) in crustaceans is one of the best-characterized oscillatory neural networks (Selverston and Moulins 1985; Marder 1997; Selverston 2010). The pyloric

circuit innervates muscles that control the region of the stomach known as the pylorus. It produces a triphasic motor pattern that consists of a burst of action potentials from the pyloric dilator (PD) neurons, followed by a burst from the lateral pyloric (LP) neuron, then by a burst from the pyloric (PY) neurons. The stomatogastric ganglion (STG) contains a small number of neurons that are consistently identifiable across animals, and it produces reliable, rhythmic electrical activity for up to several days or weeks *in vitro*. This system has been used in network-level and single-cell studies of homeostatic regulation (Marder and Bucher 2007). Several studies have shown that neuronal activity is governed in part by the maximal conductances (henceforth referred to simply as "conductances") of specific ion channel types, but the manner in which they do so is highly nonlinear. In certain instances, a small change in one conductance results in a large change in electrical activity (Goldman et al. 2001). Conversely, many different sets of ionic conductances can result in similar neural activity (Prinz et al. 2004; Schulz et al. 2006; Achard and De Schutter 2006; Swensen and Bean 2003, 2005). Of particular interest is the role of correlations between sets of ionic conductances (Khorkova and Golowasch 2007) and ion channel mRNA levels (Tobin et al. 2009) in preserving neural activity. Overexpression of the transient potassium current (I_A) in lobster STG neurons elicits an increase in the hyperpolarization-activated mixed-ion current (I_h), with minimal changes in electrical activity (MacLean et al. 2003, 2005), suggesting that a neuron can actively modify its membrane properties in order to regulate its electrical output. Computational studies scanning the conductance space of model neurons have also found that pairwise co-regulation of conductances can preserve certain aspects of neural activity (Ball et al. 2010; Hudson and Prinz 2010). The presence of these correlations suggests that the neuron is following a set of biological "rules" which are necessary for it to maintain a homeostatic equilibrium.

Much of the work on the pyloric circuit has focused on the relationships between bursts in the various neurons in the network. Previous studies have shown that pyloric burst phases are relatively invariant over time (Hooper 1997a; b), suggesting that the burst phase holds some functional importance to the pyloric rhythm. The mechanism by which the neuron accomplishes burst phase maintenance has not been resolved. Relatively little work has been done to elucidate the role of intra-burst spike patterns. It was originally believed that the spike timing within a burst played a less critical role than the timing of slow-wave oscillations in governing network activity (Raper 1979; Graubard 1978). However, recent studies have suggested that certain intra-burst properties, such as spike frequency and the number of spikes per burst, have significant effects on muscle response (Morris and Hooper 1997; Morris et al. 2000; Hooper and Weaver 2000). Other experiments have demonstrated the presence of synaptic modulation of precise spike patterns within bursts (Szucs et al. 2003; Brochini et al. 2011), and these spike patterns may have some functional significance. Furthermore, modeling studies have suggested that network responses are sensitive to these spike patterns (Latorre et al. 2006).

In this work, the relationship between spike delay and period was quantified in the crab STG. We observed that spike delays within pyloric bursts can vary proportionally with period, so that the phases of the spikes, relative to the beginning of the burst, are invariant to the period. We hypothesized that pairwise conductance correlations may be associated with this maintenance of spike phase. To test this hypothesis, two separate computational studies were performed. The first study altered the conductances of a "canonical" burster, two at a time, to determine the effects on that burster's activity. We refer to this as the "single-burster" study. An advantage to varying only two conductances at a time is that a large number of simulations can be run in two-dimensional conductance space, providing us with a high-resolution view of the pairwise relationships. A disadvantage to this approach is that the results involve modulating the parameters of a single, arbitrarily chosen burster; they thus do not constitute a comprehensive view of how spike phase is maintained in the eight-dimensional conductance space of the model neuron. The second study provides a view of this conductance space by using a model neuron database, in which all eight conductances are allowed to vary freely, to develop populations of bursters with low spike phase differences relative to one another. These populations' conductance distributions were examined over all 28 pairwise combinations of the eight conductances. We refer to this as the "population" study. The first study asks, "If six of eight of a model neuron's conductances are constrained, can the neuron preserve its activity by co-modulating the other two conductances?" The second study asks an inverse question: "If we extract from a database a population of model neurons constrained to a specific type of activity, do the pairwise distributions of their conductances suggest that the co-modulation of certain conductance pairs is needed to preserve their activity type?" The two studies complement each other, and we found that certain conductance correlations were evident in both approaches.

2 Methods

2.1 Experimental studies

Jonah crabs (*Cancer borealis*) were purchased from commercial suppliers and stored in a cold-water artificial seawater tank at ~12°C. Crab saline (11 mM KCl, 440 mM NaCl, 13 mM $CaCl_2{\cdot}2H_2O$, 26 mM $MgCl_2{\cdot}6H_2O$, 11.2 mM

Trizma base, 5.1 mM maleic acid, pH 7.45±0.03) was refrigerated until needed.

2.1.1 Preparation

The animal was cold-anesthetized for 20–30 min by submerging it in ice prior to dissection. The stomach, which includes the STNS, was removed from the animal, pinned into a deep Sylgard-lined dish, and submerged in chilled (10–15°C) saline. The STNS, including the STG and the nerves that innervate the stomach muscles, was dissected out of the stomach and pinned in fresh saline in a Sylgard-lined Petri dish. The preparation was transferred to an electrophysiology rig where fresh saline was chilled with a Peltier thermoelectric cooler and superfused over the nervous system.

2.1.2 Electrophysiology

Vaseline wells were built around the lateral ventricular nerve (lvn, which contains axons from PD, LP, and PY neurons) on each side, and a stainless steel wire electrode was placed in each well to make extracellular nerve recordings of network activity. The extracellular recording provides a convenient measure of the network cycle frequency as well as the LP neuron inter-spike intervals without having to impale multiple cells. An A-M Systems Model 1700 Differential AC Amplifier was used for extracellular recordings, and all free-running rhythm data was acquired with an Axon Instruments Digidata 1322A and pClamp 9.2 software (Molecular Devices).

2.2 Modeling studies

2.2.1 Simulation

The single-compartment conductance-based stomatogastric model neuron that was utilized to simulate neural bursting activity has been previously described (Prinz et al. 2003b). This model consists of a set of eight Hodgkin-Huxley-type ionic currents, each specified by one or two differential equations that describe voltage-dependent channel activation and inactivation. During each individual simulation, all model parameters were kept constant. The parameters in this study included eight conductance values which were taken from a model neuron database that has also been previously described (Prinz et al. 2003a). The voltage dependence and temporal dynamics for seven of these conductances were based upon *in vitro* experiments on unidentified stomatogastric cells in culture (Turrigiano et al. 1995). These conductances were: fast sodium (g_{Na}), fast transient calcium (g_{CaT}), slow transient calcium (g_{CaS}), transient potassium (g_A), calcium-dependent potassium (g_{KCa}), delayed-rectifier potassium (g_{Kd}), and a voltage-independent leak conductance (g_{leak}). Values for the eighth conductance, a hyperpolarization-activated mixed-ion inward conductance (g_H), were derived from studies on guinea pig lateral geniculate relay neurons (Huguenard and McCormick 1992).

All simulations and analysis were performed in MATLAB. Simulations were run for 20 s with a time step of 0.05 ms. Both the membrane voltage and the intracellular calcium concentrations were updated at each time step using the exponential method detailed in Dayan and Abbott (2001). Activation and inactivation variables were updated using the Euler method. Spike times were recorded at each time that the voltage made a negative-to-positive crossing over 0 mV. These spike times were then used to find which of the model neurons were stable bursters. Inter-spike intervals (ISIs) that were greater than five times the length of the previous ISI were deemed inter-burst intervals (IBIs), and the activity between the start times of two consecutive IBIs was deemed a burst cycle. After varying the threshold for classifying an ISI as an IBI between two and six times the previous ISI, we found that our chosen value of five-fold for this threshold was suitable for the present analysis. If the corresponding ISIs within each of the last three complete burst cycles differed by less than 10% from their mean, the model neuron was classified as a stable burster. Since our aim was to examine intraburst spike phase maintenance, only neurons that had reached a stable bursting pattern by the end of the simulation time were analyzed. If no IBIs were detected, according to the above criteria, the model neuron was assumed not to be a stable burster and, therefore, not to have definable intraburst spike phases. These model neurons (including silent neurons and tonic spikers) were excluded from the analysis. All regularly bursting model neurons reached stable activity well before the end of the simulation time.

2.2.2 Quantifying phase difference

To determine the effect of individually varying conductances on spike phase in the single-burster study, a "canonical" burster was first chosen, with maximal conductances shown in Table 1. This burster demonstrated steady bursting activity and a period of 0.98 s, similar to that of the pyloric rhythm typically seen *in vitro* (Marder and Bucher 2007). We then compared the spiking activity of the canonical burster to that of a "modified" burster in which one or two of the conductances were varied from the canonical value. A simple metric was used to quantify the spike phase difference between the canonical and modified bursting model neurons. If we let t_i^j denote the time of the jth spike in a regular burst from model i (spike s_i^j), where each model i's burst cycle has a period of p_i, the spike phase H_i^j of s_i^j is then defined as:

$$H_i^j = \frac{t_i^j - t_i^1}{p_i}$$

Table 1 Conductance values for the "canonical" bursting model and ranges over which they were varied in the single-burster modeling study

Conductance	"Canonical" conductance value (mS/cm^2)	Conductance range (mS/cm^2)
g_{Na}	200	0–600
g_{CaT}	5	0–15
g_{CaS}	4	0–12
g_A	40	0–120
g_{KCa}	5	0–15
g_{Kd}	125	0–375
g_H	0.01	0–0.03
g_{leak}	0.02	0–0.06

To allow spike phase comparison between models with different numbers of spikes per burst, this metric was only calculated for the first N spikes, where N denotes the lowest number of spikes between the canonical and altered bursters. The average phase difference D_i between the canonical burster and each of the altered bursters is then calculated by summing the phase differences and dividing by N-1:

$$D_i = \frac{1}{N-1}\sum_{j=1}^{N-1}\left|H_i^j - H_c^j\right|$$

where H_c^j is the spike phase for spike j of the canonical burster c. Thus, the metric D_i may be thought of as the "average phase difference per spike" relative to a canonical burster. We note that this metric ignores all spikes beyond the Nth spike. Quantifying differences in spike phase for bursters with different numbers of spikes is not trivial (Lago-Fernandez 2007). Here, we are choosing to only examine those spikes that are common to both bursters. Figure 1 illustrates the phase maintenance metric for pairs of model neurons with varying degrees of average spike phase difference. For the purposes of our computational studies, we deem any pair of model neurons with an average spike phase difference of less than 0.01 to be exhibiting high phase maintenance.

2.2.3 Data structure and statistical analysis: single-burster study

For a set of eight conductances, the number of distinct two-element subsets is given by the binomial coefficient $\binom{8}{2}$, which is equivalent to 28 possible conductance pairs. To study the effects of pairwise conductance variation on spike phase, the conductance values were independently varied, two at a time, by multiplying the canonical value by a set of multiplicative factors ranging from 0 to 3 in increments of 0.1 (see Table 1). This resulted in 31×31, or 961, combinations of values for each of the 28 conductance pairs. The average phase difference D_i per spike between each modified burster and the canonical burster was calculated. For each of these pairs of the eight conductances, two-dimensional color-coded graphs were generated by plotting the average spike phase difference versus the two conductance values. The degree of correlation between each of the two conductance pairs was quantified by identifying the subset of burster models within the 31×31 grid that exhibited a difference in phase from the canonical burster of 0.01 or less. The conductance values for those burster models that satisfied this condition were then examined for correlations using the nonparametric Spearman's rank correlation coefficient. Due to the gridlike structure of the data, using significance testing alone carries the risk of overestimating the degree of correlation. We thus define as correlated those relationships with a Spearman's rank correlation coefficient of $|\rho| \geq 0.4$ and a p-value of less than 0.05. Since our study focuses solely on examining putative monotonic relationships between conductances, we chose to perform a piecewise examination of any nonmonotonic relationships that were seen. The data was divided into approximately monotonic sections via visual inspection. We note that our method of defining the sets of bursters with high phase maintenance only considers whether $|\rho|$ is above or below the threshold; the absolute difference between the ρ value and the threshold is disregarded. However, by examining which correlations persisted as the threshold was lowered (providing a more stringent criterion for spike phase maintenance), we saw that a higher $|\rho|$ generally indicates more tightly maintained spike phases (data not shown).

2.2.4 Model neuron database

Co-varying pairs of conductances while constraining all others provides a systematic way to examine the effects of ionic currents on model neuron behavior, but only in a very localized region of conductance space. Another, more comprehensive method of examining the influence of conductance on model neuron output is through the use of a large database of model neurons, wherein all eight conductances are independently and systematically varied. Each of the model neurons in the database can then be classified based upon various features of their electrical activity, and the underlying conductances of those neuron populations that satisfy a given set of criteria (for example, bursters with a cycle period between 1 and 1.1 s) can then be examined for trends. A previously existing large model neuron database was utilized to determine whether a population of model neurons with independently varied conductance values that was constrained to regular bursters with tightly maintained spike phases would exhibit pairwise conductance correlations

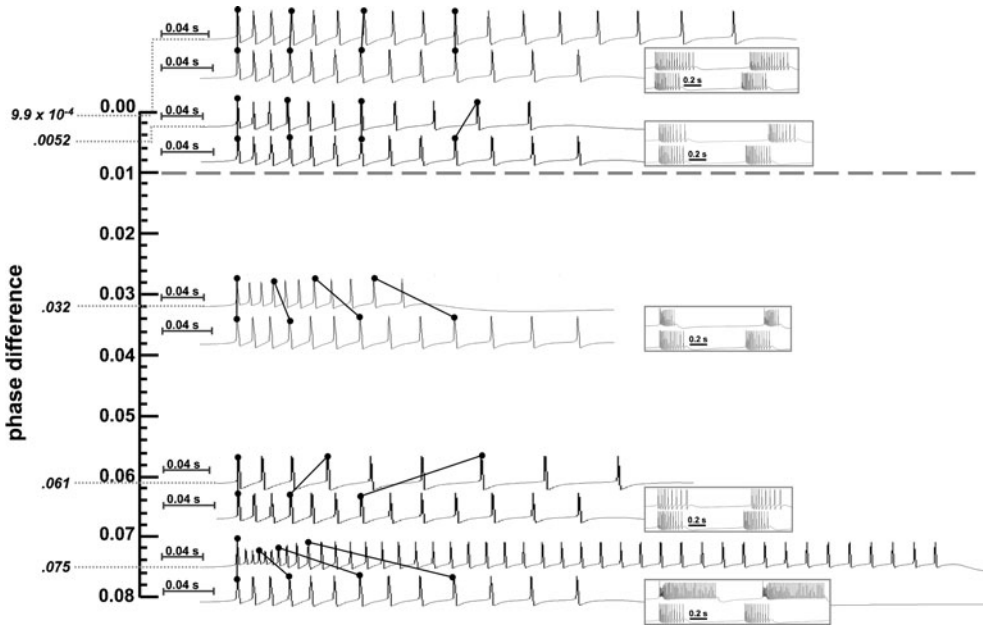

Fig. 1 Five pairs of model neuron voltage traces demonstrating progressively greater phase differences. Voltage traces were normalized by each of their respective periods; thus, the first spike of each burst is aligned. Time scale bars are shown to the left of each trace. The lower trace in each pair represents one burst from the canonical model neuron. The upper trace represents one burst from a model for which two conductances were varied from their canonical values. The black lines drawn between action potential peaks in the upper and lower traces show the divergence in phase between the first, fourth, seventh, and tenth spikes of each burster. The more vertical these lines are, the greater the maintenance of phase is between the two bursters. Traces in the insets have not been normalized by period to demonstrate the differences in the periods between the original and canonical bursters. Those pairs of model neurons with a phase difference of less than 0.01 were considered to have a high level of phase maintenance

(Prinz et al. 2003a). This database was constructed by simulating the spontaneous activity of the single-compartment conductance-based model neuron described above for six equally spaced, independently varied values of eight conductances. This resulted in 6^8, or 1,679,616, total model neurons. A variety of intrinsic activities was represented in this database, including regular and irregular spiking activity, regular and irregular bursting activity, and silence (no activity). Only those model neurons classified as regular bursters (712,613 model neurons in all) were analyzed in this study. Comparing the spike phases of neurons that burst only a few times per cycle nearly always results in a very low difference in spike phase. To avoid the possible confounding effect of low spike numbers on our results, we restricted the bursters analyzed to those with more than 4 spikes per burst.

2.2.5 Selecting model neuron populations with high and low levels of phase maintenance

From the regular bursters in the database, we selected several populations of model neurons with high phase maintenance, such that the neurons within each population had similar spike phases relative to the other neurons within the same population. To collect these populations, we constrained the duty cycle (defined as the fraction of the cycle period during which the neuron is bursting) of the model neurons to a narrow range, then restricted the number of spikes per burst to a specific value. The duty cycle is equivalent to the phase of the last spike in the burst. Because the ISIs in these bursting models generally do not exhibit large amounts of variability from model to model, constraining the phase of the last spike also constrains the phases of the other spikes in the burst. Thus, by constraining duty cycle and spike number, we obtained populations of model neurons with low phase differences relative to one another. The width of the duty cycle range is equivalent to the maximum difference that any two bursters in the population may have in the spike phase of the last spikes in their respective bursts. Thus, the average phase difference per spike within these populations is well below the width of the duty cycle range. The phases are therefore, by our definition, highly maintained in these populations; we consider them a suitable model of phase maintenance in bursting neurons. Figure 2(a) shows a sample "high phase maintenance" population of 500 bursters with duty cycles constrained between 0.06 and 0.07 and spike number constrained to 6. As a control, we also selected an analogous set of model neuron populations with low phase maintenance by constraining the period and the number of spikes per burst, but allowing the duty cycle to vary freely. A sample "low phase maintenance" population is shown in Fig. 2(b), with the period constrained between 0.70 and 0.74 s and the number of spikes per burst again constrained to 6. The

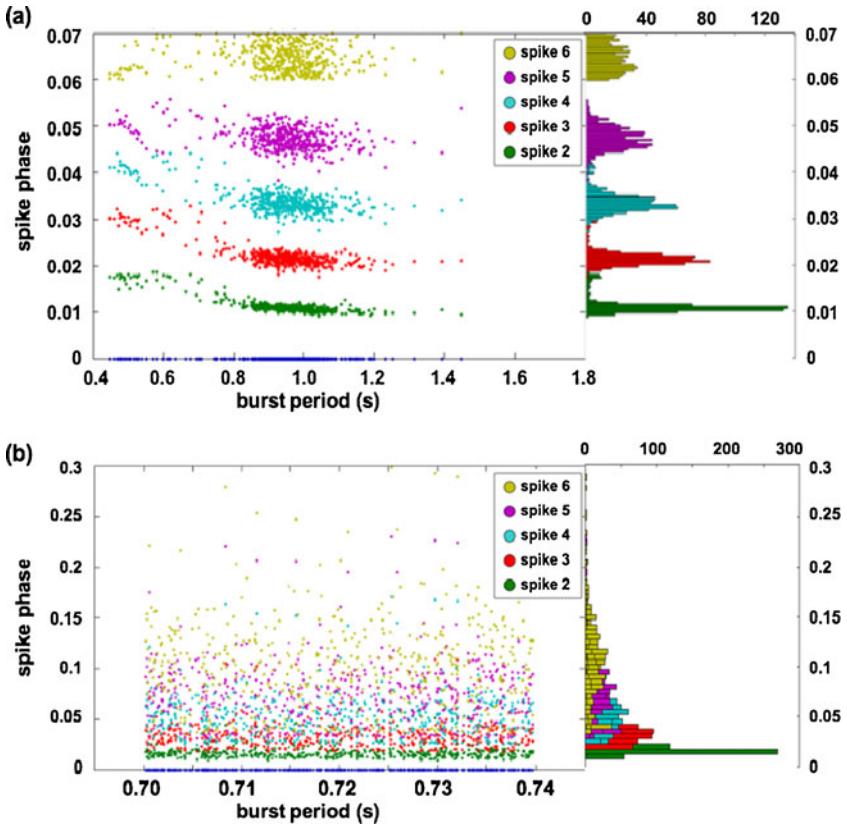

Fig. 2 Comparison of burster populations with high and low phase maintenance. (**a**) Spike phase vs. period for 500 randomly chosen bursters with 6 spikes per burst and duty cycles between 0.06 and 0.07. The period is unconstrained. Histograms (*right side of plot*) illustrate the spread of the spike phases. The narrow distributions indicate that this population exhibits high phase maintenance. (**b**) Spike phase vs. period for 500 bursters with 6 spikes per burst and periods between 0.70 and 0.74 s. The duty cycle is unconstrained. A wide distribution of spike phases indicates that this burster population exhibits low phase maintenance

variation of spike phase values in the sample "low" phase maintenance group is three- to fifteen-fold greater than in the "high" phase maintenance group, showing that their spike phase characteristics are quantifiably separable (Table S1). We then statistically analyzed the "low" and "high" phase maintenance populations for the presence of conductance correlations.

To determine whether any present correlations were an effect of constraining either the duty cycle or the spike number alone, we further selected populations of regular bursters in which either the duty cycle or the number of spikes per burst was constrained, but not both at once. The conductance correlations for all three population types (those with constrained duty cycle, constrained spike number, and constrained duty cycle and spike number) were statistically analyzed and compared.

2.2.6 Data structure and statistical analysis: population study

To check for the presence of pairwise conductance correlations, we collapsed the neuron populations down from an eight-dimensional parameter space into each of the 28 possible sets of two-dimensional space. Each of these two-dimensional distributions was then evaluated for correlations. We statistically quantified the strength of the conductance correlations in each burster subplot. One cannot assume that the model neuron output is obeying a theoretical underlying distribution, since this output has been artificially constrained. We therefore used nonparametric statistical tests as performed by Hudson and Prinz (2010). For both "high phase maintenance" and "low phase maintenance" populations, conductance pairs were deemed correlated if they met the criterion of Spearman's $|\rho| \geq 0.4$, with a p-value<0.05. We further used the nonparametric Wilcoxon rank-sum test to determine whether the sets of correlation coefficients for the two sets of model neuron populations were significantly different ($p<0.05$). For the study comparing neuron populations with constrained duty cycle and number of spikes per burst ("high phase maintenance" populations) to the populations in which only the spike number or duty cycle was constrained, two nonparametric tests, the chi-squared test of independence and the Spearman's rank correlation test, were used to determine the presence of correlations between the various pairs of conductances. Correlations were deemed present if the chi-squared statistic met the criterion of $X^2 \geq 70$ and Spearman's rank correlation coefficient met the criterion of $|\rho| \geq 0.30$. The threshold values were chosen by examining the X^2 and Spearman's ρ values for difference matrices containing visually detectable correlations. These thresholds were then universally used to test all sets of neuron populations for the presence of correlations (Hudson and Prinz 2010).

3 Results

3.1 Experimental study

We analyzed six long term recordings of the lateral pyloric (LP) neuron in the pyloric network of *Cancer borealis*. In approximately half of these recordings, the ISI varied proportionally with the burst period over time, so that spike phases were maintained. A sample preparation demonstrating this phenomenon is shown in Fig. 3(a). We plotted the delay of spikes 2–6 (relative to spike 1 of each burst) against the burst period and found a significant positive slope for all fitted trendlines (Fig. 3(b)). To quantify how close the observed spike phases were to being "perfectly" maintained, we adapted a previously described technique (Hooper 1997a). If a bursting neuron exhibits perfect spike phase maintenance, then as the burst period approaches zero, the phases of the spikes in a burst will also approach zero. Thus, plotting the spike delay relative to the beginning of the burst against the present burst period should result in a linear trendline with a positive slope and a y-intercept at (0,0). The second point that defines this "perfect delay" line must lie on the trendline that is fitted to the observed data. For each of the six preparations examined, we chose this point to be at the mean burst period for that preparation. The slope of the observed spike delay vs. period trendline for any bursting neuron should fall somewhere between zero (signifying a complete lack of phase maintenance) and the slope of the

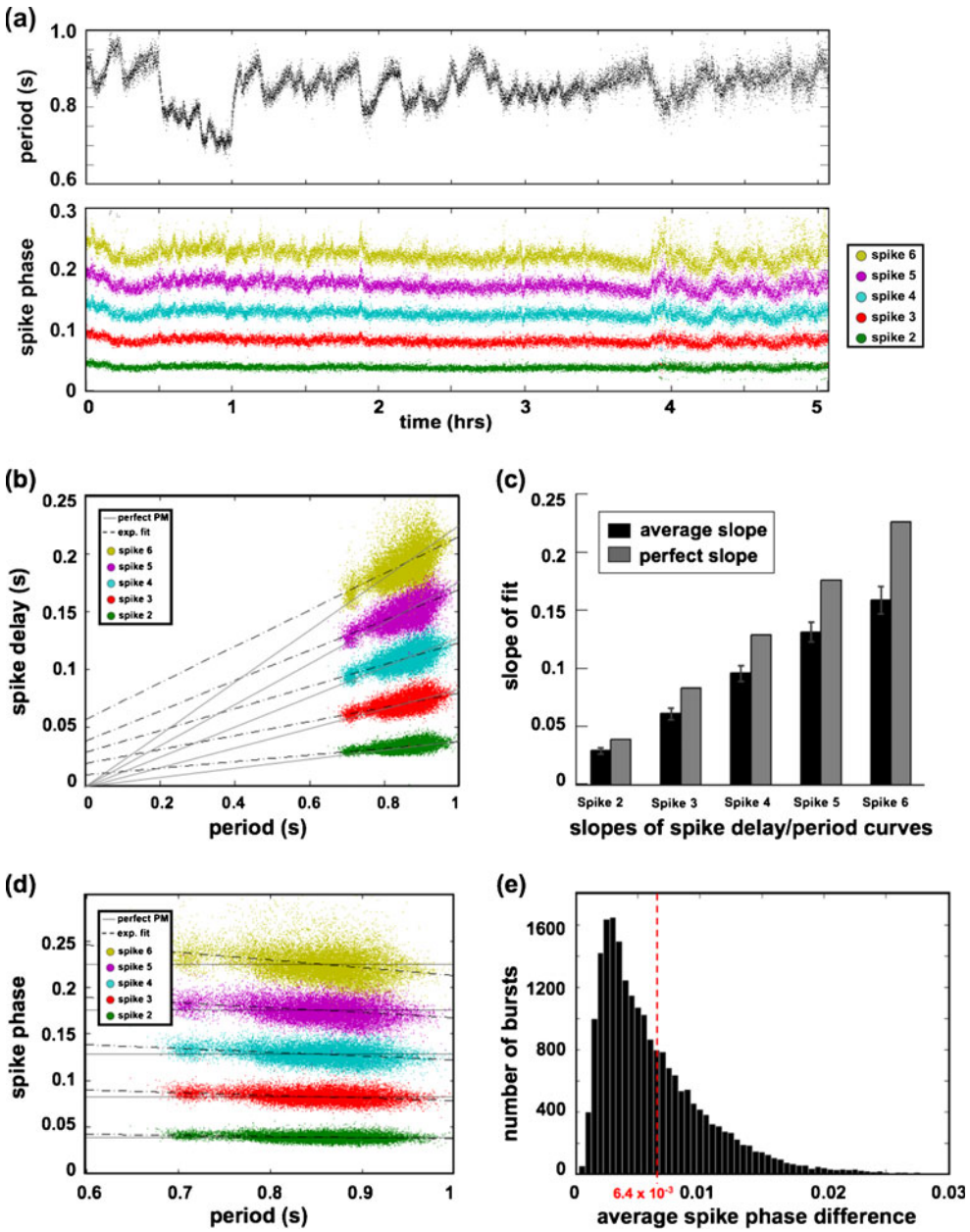

Fig. 3 Experimental data demonstrating that as period varies, spike phases can be well maintained. The pyloric rhythm from an *in vitro* preparation was recorded for approximately 5 h. (**a**) Period and spike phases for each burst are shown for the duration of the recording. (**b**) Raw data and linear fits of the delay for spikes 2–6 of each burst versus the cycle period. Each data point represents one spike. Dashed black lines ("exp. fit") indicate linear fits to the experimental data. Lines indicating perfect phase maintenance ("perfect PM") are shown in light grey. All fits have a significant positive slope. The plot is scaled to indicate the y-intercepts for each trendline. Perfect phase maintenance would correspond to lines with a y-intercept at (0,0). (**c**) The ratio of the average slope to the slope of the line indicating perfect phase maintenance ranged between 0.70 and 0.76 for spikes 2–6 in each burst. The first spike of each burst was not analyzed because its delay was defined as 0 s. (**d**) Spike phase was close to independent of the pyloric period. (**e**) Histogram showing the distribution of the average difference of the spike phases of each burst from the mean spike phases for the entire data set. The mean spike phase difference is 0.0064 (shown as *dashed red line*)

perfect delay line. A comparison of the average slope of the spike delay-burst period plot for a given neuron with the slope of perfect delay line therefore indicates the degree of phase maintenance that the neuron exhibits. For the sample experimental recording shown in Fig. 3, ratios of the slopes for the average spike delay/period trendlines to the slopes for the lines indicating perfect phase maintenance range between 0.70 and 0.76, indicating a relatively high degree of phase maintenance (Fig. 3(c)). The independence of spike phase from the period is illustrated by the horizontal trendlines in Fig. 3(d). Five other preparations were similarly examined. Of these, one exhibited ratios ranging between 0.30 and 0.51, and the other exhibited ratios between 0.73 and 1.08. Thus, three of the six preparations we examined demonstrated some degree of phase maintenance, two of them at a high and one at a moderate level. The remaining three preparations exhibited ratios near or below 0, suggesting that no phase maintenance was present.

Our metric for phase maintenance does not explicitly account for changes in period; it therefore cannot differentiate between phases that have been maintained despite large changes in period and phases that are maintained simply because other aspects of the bursting activity (period, burst duration) have been maintained, as well. For each of the preparations, we compared both the standard deviation of the periods and the percent difference between the minimum and maximum periods to the degree of phase maintenance. No relationship was detected between the amount of variation of the period (using either metric) and the degree of phase maintenance, suggesting that the presence of phase maintenance is not due to a lack of change in the period.

To determine how well the spike phases are maintained within a single preparation over time, we calculated the difference between the phase of each spike in each burst and the mean phase of that spike for all bursts in the data set shown in Fig. 3. We then averaged each burst's spike phase differences, resulting in one average phase difference for each burst in the data set. The distribution of these average spike phase differences are shown in Fig. 3(e). The mean of the average spike phase difference for each burst is 0.0064 (red dashed line). We chose to use a similar value (0.01) to define our lower limit of spike phase maintenance in the modeling studies.

3.2 Single-burster study

In the twenty-eight pairs of conductances in the single-burster study, different types of qualitative relationships were seen: monotonic, non-monotonic, and independent relationships. Figure 4(a) depicts the degree of phase difference for each of the 28 pairs of conductances, when both conductances in the pair are varied. Table 2 shows the Spearman's ρ and p-values for every pairwise correlation.

Fig. 4 Phase differences and conductance correlations in the single-burster study. (**a**) Average spike phase differences relative to the canonical burster for the pairwise co-variations of all 28 pairs of conductances. Dark blue regions have the highest phase maintenance, and dark red regions have the lowest phase maintenance. White squares indicate model neurons that were not regular bursters. Regions with low spike phase differences (<0.01) that were examined for correlations are outlined in magenta and have their grid lines in bold. Conductance data sets with nonmonotonic relationships that resulted in phase maintenance were analyzed piecewise; the divisions between these regions of analysis are indicated with straight, solid magenta lines. Bold black outlines indicate conductance pairs with positive correlations, and bold red outlines indicate conductance pairs with negative correlations. Dashed red-and-black outlines indicate the presence of both a negative and a positive correlation. (**b**) Summary of correlations seen in all 28 conductance pairs. Positive correlations are indicated by a plus sign, and negative correlations are indicated by a minus sign. Conductance correlations were deemed present if Spearman's rank correlation coefficient had a value of $|\rho| \geq 0.4$ ($p<0.05$). Blank squares indicate conductance pairs for which no correlation was found. Squares that are divided indicate nonmonotonic relationships that were analyzed in a piecewise fashion. (**c**) Original voltage traces show that positively varying g_{CaT} and g_{Kd} supports spike phase maintenance. Three pairs of voltage traces are shown whose phase differences are highlighted on the bar plot. Traces are normalized by their respective periods; the first spike of each burst is aligned. The lower trace in each pair represents one burst from the canonical model neuron, marked on the plot with a magenta square. The upper trace represents one burst from a model for which g_{Kd} and g_{CaT} varied from their canonical values. Black lines drawn between action potential peaks in the upper and lower traces show the divergence in phase between every third action potential of each burster. Traces in the insets have not been normalized by period to demonstrate the differences in the periods between the original and canonical bursters

The correlations for each conductance pair are summarized in Fig. 4(b). According to our criteria ($|\rho| \geq 0.4$, $p<0.05$), six conductance pairs had monotonic relationships that were correlated across the entire data set, and seven had non-monotonic relationships that exhibited at least one correlation when examined in a piecewise fashion. Of the monotonic relationships, five conductance pairs were positively correlated in model neuron populations exhibiting phase maintenance, and one was negatively correlated. Of the nonmonotonic relationships that were examined piecewise, three had a positively correlated and a negatively correlated component, one had two positively correlated components, and three had only one component of two that was correlated. Of all 28 conductance pairs, g_{CaT}/g_{Kd} exhibited the strongest relationship (Fig. 4(c)), with a ρ of 0.98 ($p<1.4\times10^{-45}$). Linearly varying g_{CaT} to g_{Kd} with a ratio of approximately 0.019 results in phase maintenance. Deviating from this positive ratio results in a drastic increase in the spike phase difference. Notably, these two conductances do not tightly regulate whether the neuron is bursting; as can be seen in Fig. 4(a), the model neuron bursts across wide ranges of values for both conductances. For another strongly correlated conductance pair, g_A and g_{CaS}, the conductances constrain the bursting ability of the neuron as well as the ability

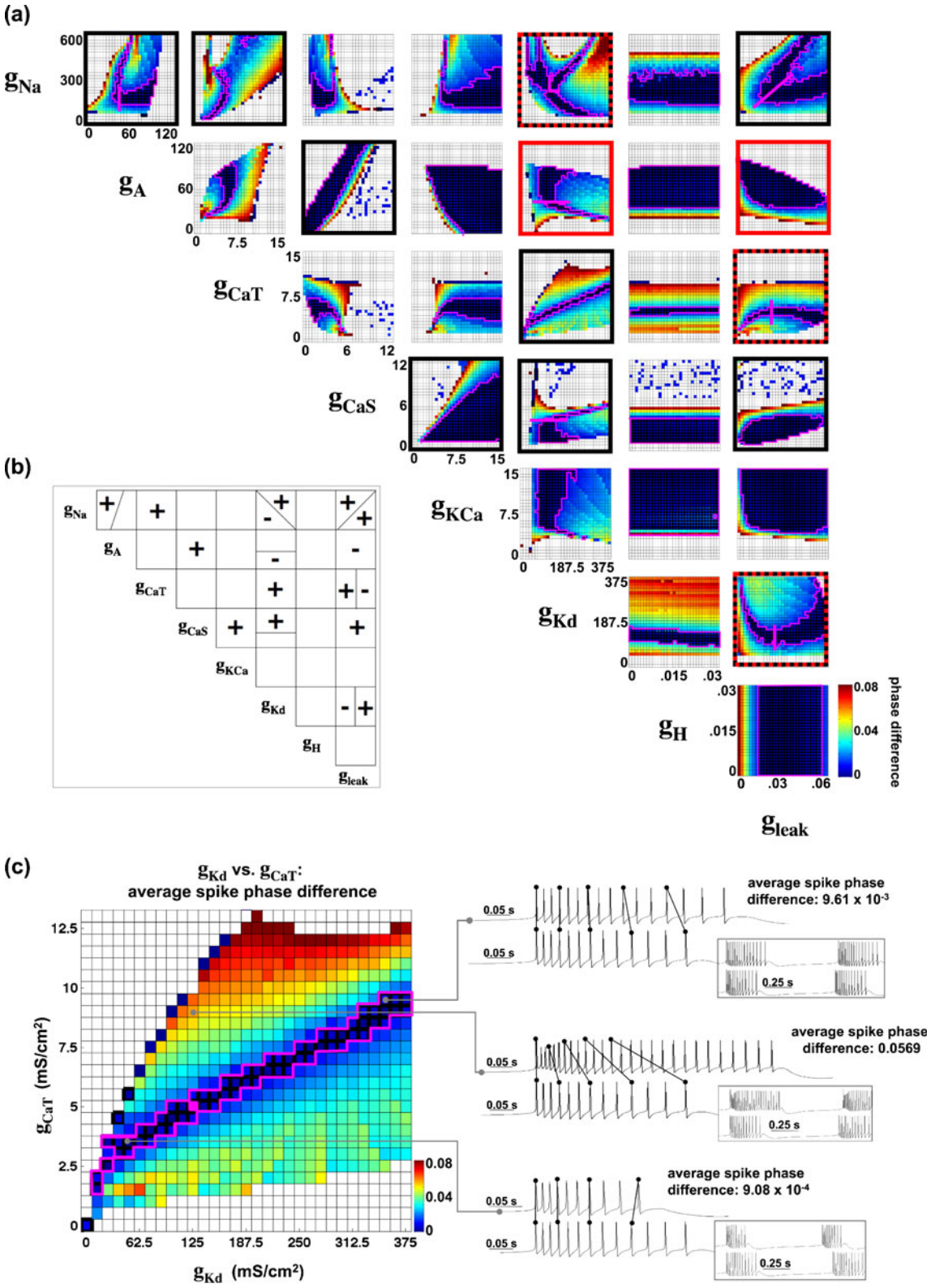

to maintain spike phase. Certain conductance pairs with nonmonotonic relationships had strongly monotonic regions that resulted in phase maintenance. The phase-maintained population for the g_{Na}/g_{Kd} pair had one region with a negative monotonic relationship ($\rho=-0.89$, $p<1\times10^{-40}$) and another region with a positive monotonic relationship

Table 2 Correlation strength of conductances from the single-burster and population studies for all conductance pairs

	Single-burster study		Population study	
Conductance Pair (g_x)	Spearman's ρ	p-value	Spearman's ρ	X^2
g_{CaT} vs. g_{Kd}	*0.98 (+)*	*1.36×10^{-46}*	0.47	60.1
g_A vs. g_{CaS}	*0.92 (+)*	*7.27×10^{-89}*	0.04	37.7
g_{Na} vs. g_{CaT}	*0.69 (+)*	*2.04×10^{-07}*	*0.8*	*264.2*
g_{CaS} vs. g_{leak}	*0.51 (+)*	*3.91×10^{-14}*	0.2	34.4
g_{CaS} vs. g_{KCa}	*0.44 (+)*	*$<1\times10^{-90}$*	*0.67*	*177.7*
g_{CaT} vs. g_H	0.36	0.00	−0.03	25.7
g_{Kd} vs. g_{leak}	*0.62 (+,R)* *−0.87 (−,L)*	*0.00* *9.95×10^{-19}*	−0.15	40.4
g_A vs. g_{CaT}	0.3	0.01	0.24	38.2
g_{KCa} vs. g_{Kd}	0.2	0.01	0.12	40.4
g_{Na} vs. g_{leak}	*0.53 (+,BR)* *0.94 (+,TL)*	*1.39×10^{-11}* *6.75×10^{-51}*	−0.18	23.0
g_{Na} vs. g_{KCa}	0.16	0.03	−0.36	62.7
g_{CaS} vs. g_{Kd}	−0.26 *0.98 (+,T)*	0.04 *4.34×10^{-12}*	−0.2	23.0
g_A vs. g_H	0.02	0.64	0.11	22.4
g_{KCa} vs. g_H	0	0.95	−0.07	19.6
g_{CaS} vs. g_H	0	1.00	0	18.5
g_H vs. g_{leak}	0	1.00	−0.05	45.1
g_{Na} vs. g_H	−0.03	0.58	−0.13	25.1
g_{Na} vs. g_{CaS}	−0.06	0.65	−0.27	37.6
g_{Na} vs. g_A	*0.94 (+,TL)* 0.07	*1.15×10^{-14}* 0.50	0.27	31.5
g_{KCa} vs. g_{leak}	−0.07	0.09	−0.09	26.3
g_{CaT} vs. g_{KCa}	−0.12	0.16	*−0.52*	*81.8*
g_{CaT} vs. g_{leak}	*0.89 (+,L)* *−0.55 (−,R)*	*1.65×10^{-07}* *4.42×10^{-07}*	−0.02	40.0
g_A vs. g_{Kd}	0.24 *−0.57 (−,B)*	0.02 *0.00*	−0.16	34.3
g_A vs. g_{KCa}	−0.27	2.90×10^{-09}	*−0.37*	*78.2*
g_{CaT} vs. g_{CaS}	−0.37	0.01	*−0.47*	*71.7*
g_{Kd} vs. g_H	−0.39	2.27×10^{-06}	−0.11	16.9
g_{Na} vs. g_{Kd}	*0.94 (+,TR)* *−0.90 (−,BL)*	*1.94×10^{-45}* *3.92×10^{-20}*	0.22	31.8
g_A vs. g_{leak}	*−0.55 (−)*	*0.00*	−0.16	41.9

Columns 2 and 3 show the statistical output from the single-burster study, in which conductances were varied pairwise by a multiplicative factor of 0 to 3 from a canonical value. Pairs are sorted by their Spearman's ρvalues (column 2). For those conductance pairs with relationships that were examined piecewise, statistical output is shown from each portion of the data. To indicate which portion is being referred to, the relative locations of the respective portions of data are indicated in parentheses (*L* left, *R* right, *T* top, *B* bottom, *TL* top left, *BL* bottom left, *TR* top right, *BR* bottom right). Columns 4 and 5 show the statistical output from the population study, in which a population of model neurons constrained to have a duty cycle of 0.2784± 0.005 and 13 spikes per burst was examined for conductance correlations. Values are italicized if both criteria for correlation are met ($|\rho|\geq0.4$, $p<0.05$ for the single-burster study, and $|\rho|\geq0.3$ and $X^2\geq70$ for the population study)

($\rho=0.93$, $p<1\times10^{-10}$). Other pairs of conductances only exhibited correlations in certain regions of conductance space. Both the g_A/g_{Kd} pairs and the g_{CaS}/g_{Kd} pairs, for example, only exhibit correlations for higher values of g_{Kd}. The conductance that appeared to least affect average spike phase difference was g_H; no correlations of g_H with other conductances resulted in populations with spike phase maintenance.

Our criteria for a conductance relationship to be deemed a correlation included a minimum value for Spearman's ρ. Excluding this criterion would cause nine other pairs of conductances to appear correlated in the phase-maintained model neuron populations (Table 2). Some, such as the g_{Kd}/g_H pair, appear only weakly correlated. We have restricted our discussion to those relationships with a higher ρ, but we note that relaxing this criterion unmasks several weaker correlations that also modestly affect spike phase maintenance.

We examined the variation in period over the ranges of conductance values (data not shown); as with the experimental data, a strong relationship between spike phase maintenance and period maintenance does not appear to exist. Figure 1 shows, for example, that the pairs of bursters exhibiting average spike phase differences of 0.0052 (a low value) and 0.075 (a high value) have similar differences in

period. To see whether our choice of aligning bursts by their first spike affected our findings, we also examined the phase differences after aligning all bursters by their last spike. The phase differences were generally greater when using last-spike alignment, which may arise in part from the differing degrees of spike frequency adaptation at the ends of the bursts (Fig. S1). However, the correlations that resulted were highly similar to those found using first-spike alignment, suggesting that the overall relationship between phase maintenance and ion channel correlations is not localized to particular regions of the burst, but is generalizable to the nature of the burst as a whole.

3.3 Population study

The method of analysis used in the single-burster study only considers a very restricted region of conductance space, in which two of eight conductances are varied at one time. The second study, utilizing a large model neuron database, allowed all conductances to vary freely. Rather than plotting the phase differences between sets of models, we plotted two-dimensional histograms to determine whether certain pairs of conductances tended to vary together in a large model neuron population with a high degree of phase maintenance.

3.3.1 Histograms and difference matrices for a sample burster population

For each pair of conductances (28 in total) and each burster population, a 6-by-6 two-dimensional histogram was generated, plotting the number of model neurons in the subpopulation versus two of their conductance values. However, the two-dimensional histograms do not explicitly account for the null hypothesis of independence between the two conductances' effects on bursting activity. To correct for this, a set of "expectation matrices" was generated (Hudson and Prinz 2010). These matrices are developed by multiplying the one-dimensional histograms for each single conductance together, then normalizing by the total number of model neurons in the population, to create a six-by-six grid of probability values. Each value represents the probability of a model neuron from the population being present in that bin, given the assumption that the two conductances are independent from one another. A set of "difference matrices," in which we subtracted the expectation matrix from the original two-dimensional histogram, was then plotted. In these plots, each bin illustrates the percentage difference between the expected value for the number of model neurons in that bin, given the assumption of independence between the conductances, and the actual value. To compare this method of examining model neuron populations to our original method of examining a single canonical burster, we first examined the conductance correlations of a population that included the canonical burster (Fig. 5). This population was constrained to include 13 spikes per burst, and its duty cycle range was allowed to vary by ±0.005 from the canonical burster's duty cycle. By restricting the duty cycle to a range of 0.01, we guarantee that the average spike phase difference is less than this value. The correlations for the single-burster study are shown with the conductance correlations from the population study in Table 2.

The correlations calculated from phase difference (single-burster study) and the correlations calculated from the histograms (population-based study) both point to phase-maintaining relationships between the sodium conductance (g_{Na}) and transient calcium conductance (g_{CaT}), as well as between the slow calcium conductance (g_{CaS}) and calcium-dependent potassium conductance (g_{KCa}). According to our criteria, the population study does not explicitly show a correlation between the transient calcium conductance (g_{CaT}) and the delayed rectifier conductance (g_{Kd}), but Table 2 shows that the relationship is comparably strong. The agreement between the two studies regarding the significance of these three conductance pairs suggests that they may play a role in spike phase maintenance in different regions of conductance space. There was no agreement between the two studies regarding which conductance pairs had negative conductance correlations that resulted in phase maintenance.

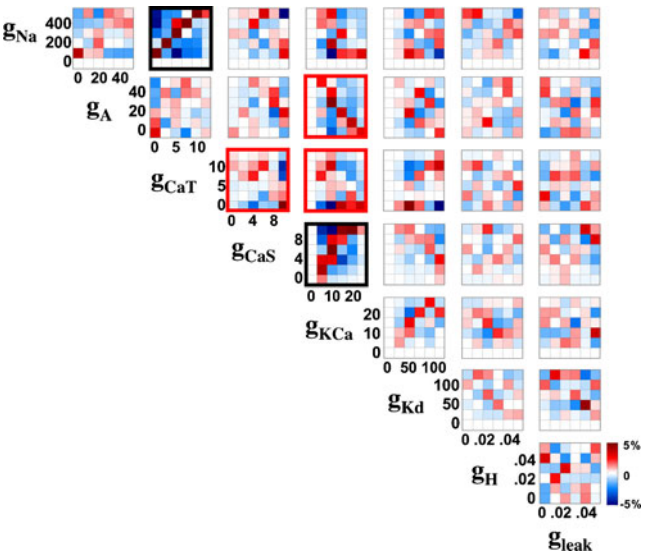

Fig. 5 Difference matrices showing the presence of correlations between certain pairs of conductances (in mS/cm^2)for a burster population exhibiting a high level of phase maintenance. This population was chosen such that the canonical burster from the single-burster study would be included; the duty cycle was restricted to 0.2784±0.005, and the number of spikes was restricted to 13 per burst. Bold black outlines indicate conductance pairs with positive correlations, and red outlines indicate the pairs that demonstrate a negative correlation

3.3.2 Comparison of several burster populations

In order to generate a single difference matrix, it is necessary to choose a single, arbitrary duty cycle range and number of spikes per burst. To further determine whether certain conductance correlations are consistently associated with phase maintenance for a variety of duty cycles and numbers of spikes per burst, we next examined several neuron populations in a similar fashion to the sample model neuron population discussed above. We investigated these sets of model neuron populations in two ways. First, we compared a set of model neuron populations with "high phase maintenance" to a set of populations with "low phase maintenance." Secondly, we compared the "high phase maintenance" populations, in which both duty cycle and number of spikes per burst were constrained, to analogous populations for which either the duty cycle or spike number was constrained, but not both. Conductance correlations that are present in the model neuron population exhibiting high phase maintenance, but not in the population exhibiting low phase maintenance or in the populations with only the duty cycle or spike number constrained, are specifically associated with maintaining phase.

3.3.3 "High" versus "low" phase maintenance populations

The "high phase maintenance" model neuron populations had spike numbers ranging from 5 to 20 and duty cycle ranges of 0.01 units in width ranging from 0.10–0.11 to 0.69–0.70. This resulted in 960 separate "high phase maintenance" populations. The "low phase maintenance" model neuron populations had spike numbers ranging from 5 to 20 and period ranges of 0.01 s in width, ranging from 0.5–0.51 s to 1.09–1.1 s, resulting in 960 "low phase maintenance" populations.

Histograms of the correlation coefficients for the populations of model neuron bursters with "high" and "low" phase maintenance were plotted for each of the 28 pairs of conductances, five of which are shown in Fig. 6. For certain pairs, the correlation coefficients appear stronger for the population representing high phase maintenance than for the

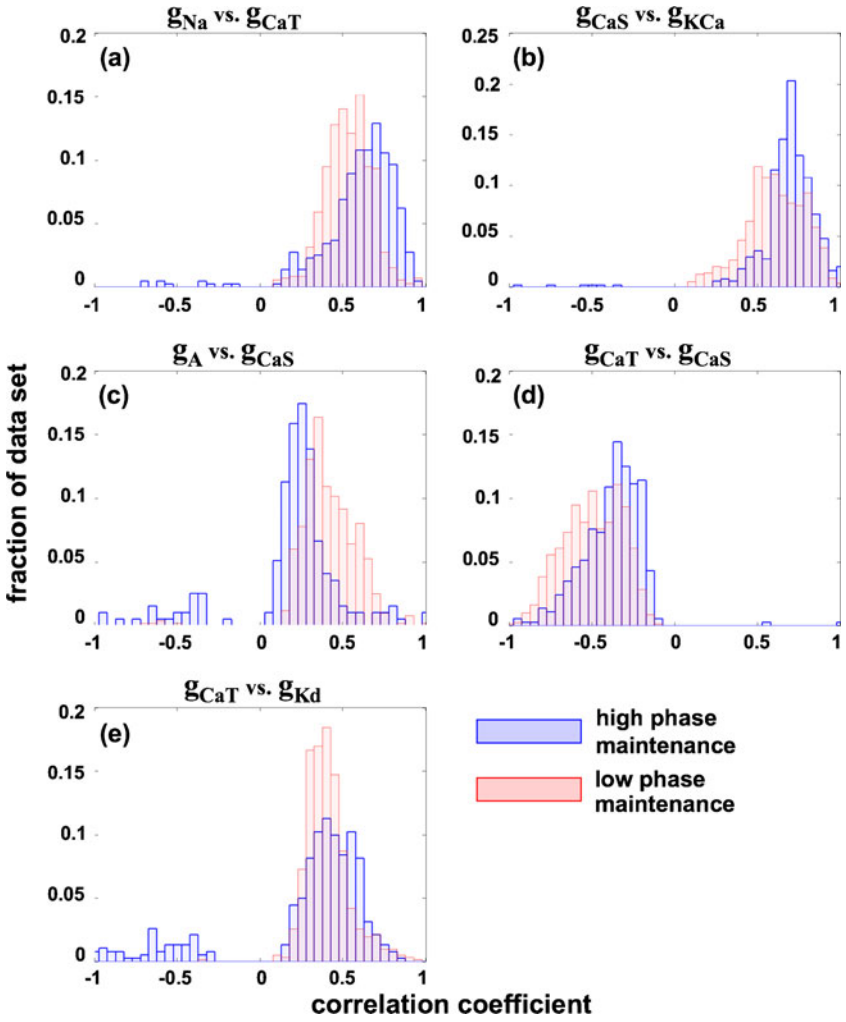

Fig. 6 Histograms of conductance correlation coefficients for a selection of conductance pairs. The y-axis indicates what fraction of the entire data set each bin constitutes. Populations of bursters with a high degree of phase maintenance are shown in blue, and burster populations that emulate a lack of phase maintenance are shown in red. (**a**) g_{Na} and g_{CaT} ($p=1.5\times10^{-20}$) and (**b**) g_{CaS} and g_{KCa} ($p=6.37\times10^{-19}$) demonstrate positive correlations that were significantly stronger (Wilcoxon rank-sum test, $p<0.05$) in the population with high phase maintenance than in the population with low phase maintenance. Conversely, the conductance pairs (**c**) g_A and g_{CaS} ($p=1.1\times10^{-33}$) and (**d**) g_{CaT} and g_{CaS} ($p=5.9\times10^{-24}$) demonstrated a significantly greater correlation in the population with low phase maintenance than in the population with high phase maintenance. (**e**) The g_{CaT}/g_{Kd} correlation coefficients demonstrated no difference between the populations with high and low phase maintenance ($p>0.05$)

population representing low phase maintenance (g_{Na}/g_{CaT}, g_{CaS}/g_{KCa}, Fig. 6(a)–(b)). This suggests that correlating these particular conductances may aid specifically in the maintenance of spike phase. Certain other pairs, however, saw stronger correlations in populations with low phase maintenance (g_A/g_{CaS}, g_{CaT}/g_{CaS}, Fig. 6(c)–(d)). Other correlation coefficients do not appear to be specifically high for the population of neurons exhibiting high levels of phase maintenance, relative to those exhibiting low phase maintenance (g_{CaT}/g_{Kd}, Fig. 6(e)).

To ensure that the correlations seen were not a result of the initial restriction of the database to all regular bursters, pairwise correlations were calculated for several populations of 10,000 randomly chosen regular bursters (Fig. S2). No strong correlations were evident in these populations, suggesting that restricting the neuronal activity type to bursting does not, by itself, result in the emergence of strong conductance correlations.

3.3.4 Effect of constraining duty cycle or spike number alone

In order to compare the "high phase maintenance" populations with those populations in which only the duty cycle or the number of spikes per burst was constrained, two additional sets of populations were generated, one with the duty cycle constrained to a range of 0.01, and one with the number of spikes per burst constrained to a single integer value. Again, the model neuron populations had spike numbers ranging from 5 to 20 and duty cycle ranges of 0.01 units in width ranging from 0.10–0.11 to 0.69–0.70. To ensure that an adequate number of model neurons were present in the histograms (each of which consisted of a 6-by-6 grid), only those bins containing at least 200 model neurons were considered. This limited the analysis to 147 populations. The three sets of burster populations (those with a constrained duty cycle, a constrained spike number, and both a constrained duty cycle and spike number) were collected as follows. Exactly 200 model neurons were chosen from each of the 147 burster populations that were constrained by duty cycle and spike number and contained at least 200 bursters (Fig. 7(a)). Next, 147 populations consisting of exactly 200 model neurons that were constrained only by duty cycle were extracted by randomly selecting from all model neurons with a specific number of spikes per burst (Fig. 7(b)). The distribution of the duty cycle bins from which these populations were chosen was designed to match that of the populations constrained by both duty cycle and number of spikes per burst. For example, since there are three populations of at least 200 model neurons with 15 spikes per burst and some specific duty cycle range (outlined in red in Fig. 7(a)), three model neuron populations of 200 randomly chosen model neurons with an unconstrained duty cycle

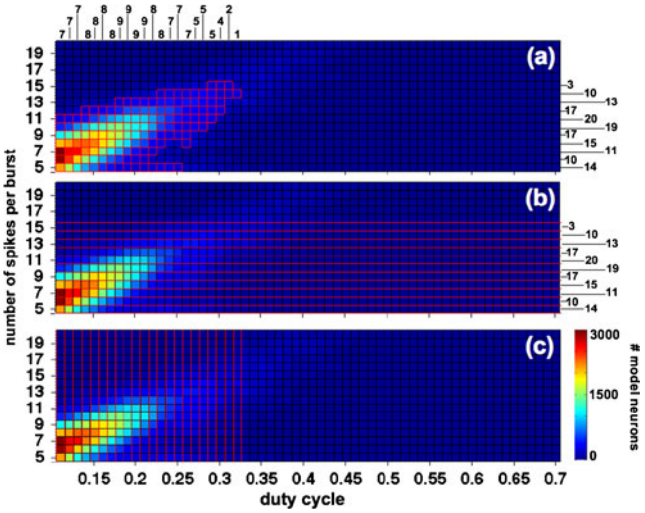

Fig. 7 Histogram depicting the number of model neurons in each of the 960 bins selected by constraining the duty cycle and number of spikes per burst of model neurons in the database. To assess the relationship of conductance correlations to spike phase maintenance, model neuron populations were collected by constraining by duty cycle and number of spikes per burst, duty cycle alone, and number of spikes per burst alone. Model neurons were partitioned by duty cycle into bins of width 0.01 and by integer numbers of spikes per burst. (**a**) Bins outlined in red indicate populations constrained by both duty cycle and spike number that are also of a size greater than or equal to 200, fulfilling our criteria for analysis. (**b**) Populations of 200 randomly selected bursters were gathered from sets of data outlined in red, wherein the number of spikes per burst, but not duty cycle, was constrained. The number of populations from each set of data is indicated on the right of the panel. (**c**) Populations of 200 randomly selected bursters were gathered from sets of data outlined in red, wherein the duty cycle, but not the number of spikes per burst, was constrained. The number of populations from each set of data is indicated above the top panel

were also chosen from this bin, so that all of the model neurons in each of the three populations had 15 spikes per burst. A similar procedure was undertaken for selecting the 147 populations of bursters with a constrained duty cycle range (Fig. 7(c)). The X^2 and Spearman's ρ values of these three sets of 147 burster populations were then compared. Bar plots showing the percentage of model neuron populations with correlated conductance pairs were compared for the three types of populations (Fig. 8), for all 28 conductance pairs. If a greater percentage of the populations with both duty cycle and spike number constrained had correlations than did those populations with either duty cycle or spike number constrained alone, it would suggest that spike phase maintenance, by our definition, is regulated by that particular conductance pair.

For the sodium and transient calcium conductances, 76% of the populations with a high degree of phase maintenance exhibited correlations, where both the duty cycle and number of spikes per burst were constrained. Of those populations with constrained duty cycle or constrained numbers of

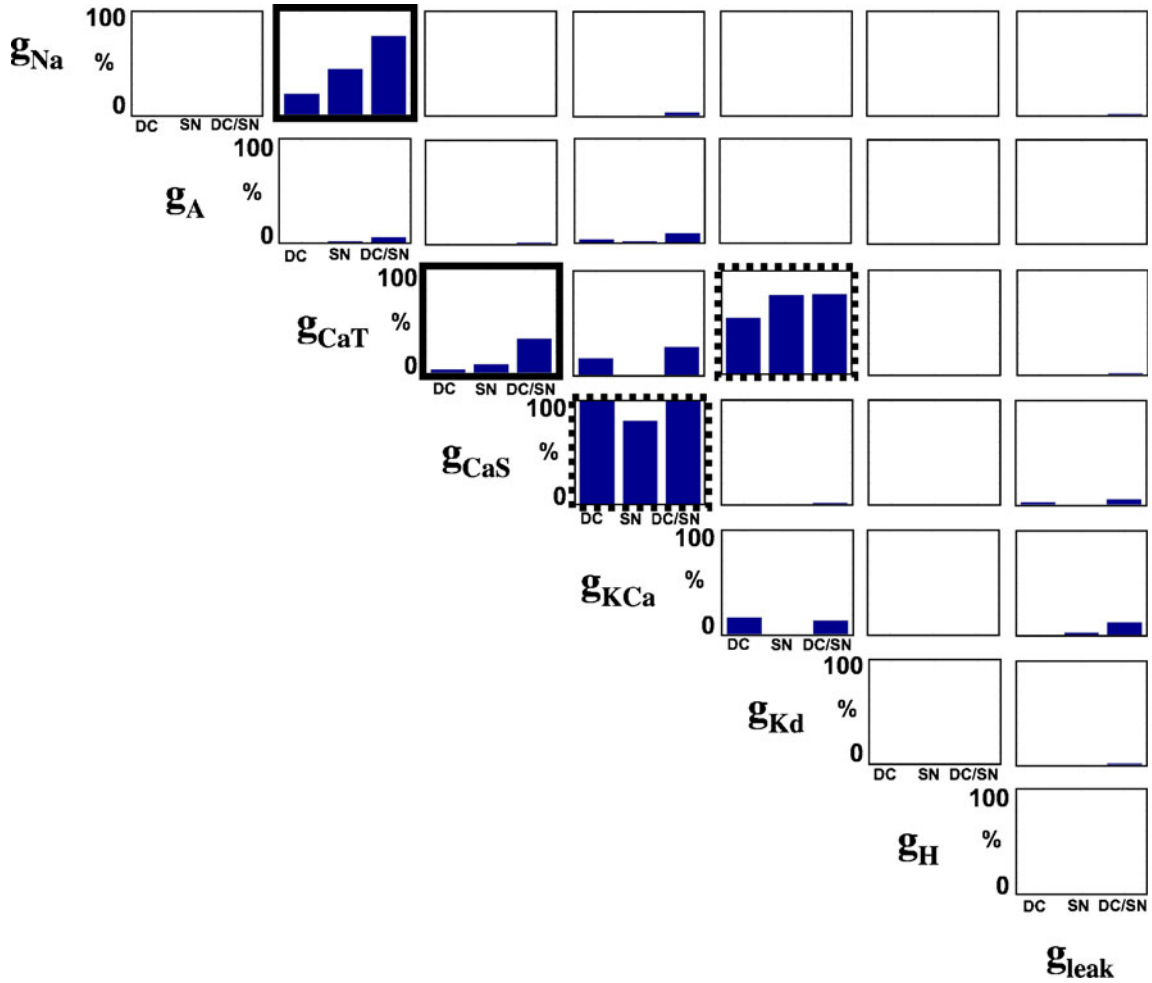

Fig. 8 Percentage of model neuron populations that meet the criteria for significantly correlated conductances ($X^2 \geq 70$ and Spearman's $|\rho| \geq 0.30$). Bars indicate populations with constrained duty cycle (DC), constrained number of spikes per burst (SN), or with both constrained duty cycle and number of spikes per burst (DC/SN). Conductance correlations that appear specifically related to maintaining phase include g_{Na}/g_{CaT} and g_{CaT}/g_{CaS} (*solid bold outlines*). Correlations between g_{CaS}/g_{KCa} and g_{CaT}/g_{Kd} pairs (*dashed outlines*) are seen in all three types of populations

spikes per burst alone, 20% and 44% appeared to have strong correlations, respectively. Thus, the g_{Na}/g_{CaT} pair may be specifically involved in maintaining spike phase. Similarly, for the g_{CaT}/g_{CaS} pair, 33% of the populations with a high degree of phase maintenance exhibited correlations, while only 3% and 8% of those populations with constrained duty cycle or constrained numbers of spikes per burst alone exhibited correlations. The g_{CaS}/g_{KCa} pair also exhibited a high number of strong correlations, but the percentages of strong correlations in each of the three sets of populations were similar, suggesting that this pair of conductances may be involved in maintaining one parameter or the other but is not exclusively associated with the maintenance of spike phase in bursting neurons. Table S2 shows the percentages of populations with correlated conductances for all 28 conductance pairs.

It is possible that the duty cycle bin size (here, arbitrarily chosen to be 0.01 units in width) may affect whether correlations are present. We performed the above study using various bin sizes and found that as long as the bins are sufficiently small, their width does not greatly affect the strength of the correlation coefficients (Table S3).

The box plots for the g_{Na}/g_{CaT} conductance pair (Fig. 9) and the g_{CaT}/g_{CaS} conductance pair (Fig. 10) illustrate stronger chi-squared values in the population exhibiting high phase maintenance. In the g_{Na}/g_{CaT} pair, the chi-squared values also appear to increase in strength as both the duty cycle and number of spikes per burst increase. This increase is most striking in the population with both parameters constrained. In the g_{CaT}/g_{CaS} pair, the populations with both parameters constrained have greater chi-squared values than the populations with only duty cycle or spike number constrained for the majority of duty cycle ranges and particularly at low numbers of spikes per burst. For both pairs, the Spearman's ρ values are similar for all three population types (duty cycle and spike number constrained, duty cycle

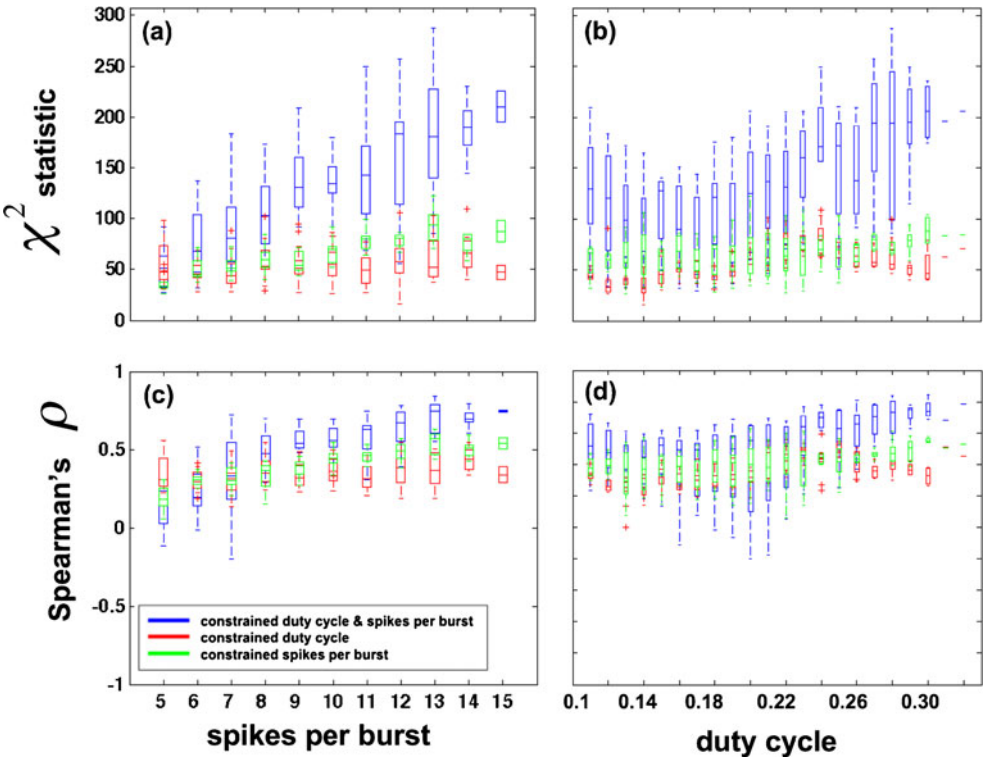

Fig. 9 Chi-squared and Spearman's ρ values for the g_{Na}/g_{CaT} conductance correlation for the three population types, plotted by number of spikes per burst and duty cycle. The line bisecting each box indicates the median values for the statistic, and the ends of the boxes indicate the lower and upper quartiles. (**a**) As the number of spikes per burst is increased, stronger correlations are seen specifically for the population of bursters with both constrained duty cycle and spikes per burst. (**b**) Stronger correlations are also seen as the duty cycle is increased. (**c–d**) Spearman's ρ values are similar between all three population types for a range of values for duty cycle and spikes per burst. For the g_{Na}/g_{CaT} conductance pair, the population wherein the spike number and duty cycle are constrained (the "high phase maintenance" population) exhibits stronger correlations than the populations in which either parameter is constrained alone

constrained only, and spike number constrained only). Thus, for the g_{Na}/g_{CaT} and g_{CaT}/g_{CaS} conductance pairs, a stronger dependence exists between the conductances (indicated by the chi-squared value) for the population with both constrained duty cycle and spike per burst (representing high phase maintenance), but the monotonicity (indicated by ρ) is similar for all population types. The box plot for the g_{CaS}/g_{KCa} conductance pair shows that the correlations are similar for all three of the sets of populations, suggesting that this particular conductance pair may be involved in constraining duty cycle or spike phase, but is not exclusively involved in maintaining both at once (Fig. 11).

4 Discussion

It is often assumed that for any nervous system to consistently produce behavior that is appropriate to the animal's environment, certain aspects of that nervous system must be held under tight neuromodulatory, cell-intrinsic, or synaptic control. In the present work, we observed through experiment that spike phase maintenance occurs in long-term recordings of some LP neurons as the period varies over time. We performed a series of studies using a single-compartment neuron model to examine whether the experimentally observed activity could be emulated via the pairwise co-variation of conductances. We first studied the effect on phase maintenance of independently varying pairs of conductance values of a single, "canonical" model neuron. Next, we utilized a model neuron database to explore whether the distributions of the conductance values of model neurons are associated with spike phase maintenance. Conductance-based modeling studies implicated the correlation of specific conductance pairs as a possible mechanism by which the pyloric neurons accomplish spike phase maintenance.

The g_{Na}/g_{CaT} pair and the g_{CaS}/g_{KCa} conductance pair exhibited salient positive correlations in the single-burster and the population-based study. Of these pairs, g_{Na} and g_{CaT} appeared more specifically geared towards maintaining spike phase than maintaining other bursting properties, such as duty cycle or number of spikes per burst alone, while the g_{CaS}/g_{KCa} pair appears to support more general bursting properties. Hudson and Prinz (2010) have also previously

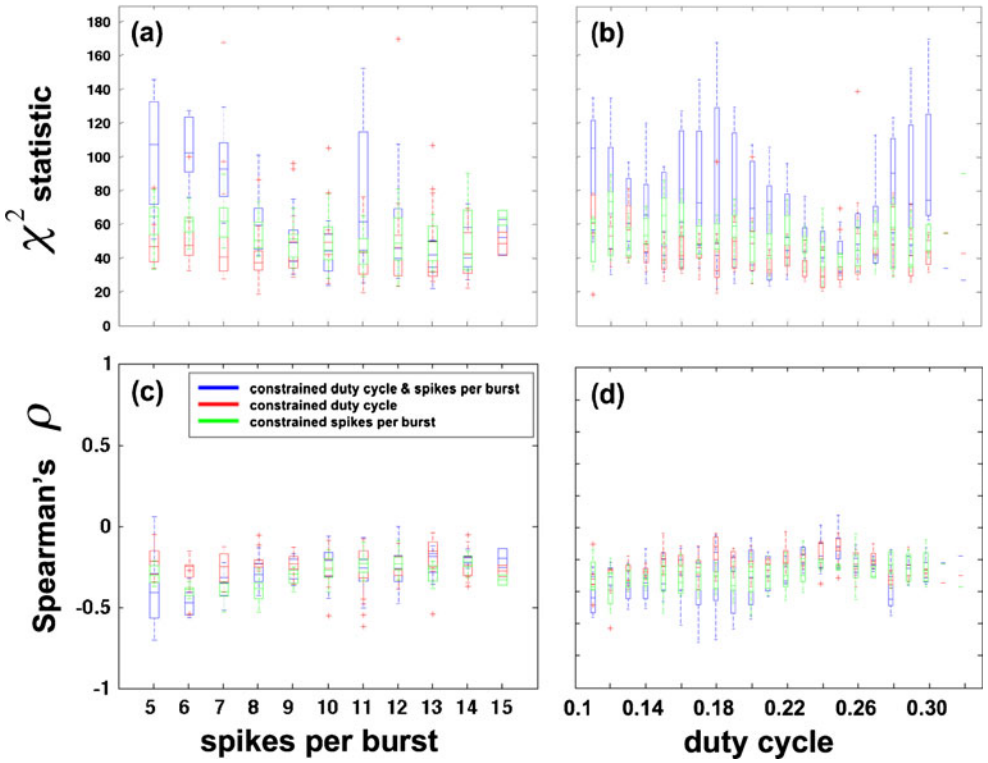

Fig. 10 Chi-squared and Spearman's ρ values for the g_{CaT}/g_{CaS} conductance pair for the three populations, plotted by number of spikes per burst and duty cycle. The middle of the boxes indicates the mean values for the statistics, and the ends of the boxes indicate the lower and upper quartiles. (**a**) At lower numbers of spikes per burst, the population with both duty cycle and number of spikes per burst constrained (in blue) has higher chi-squared values than the populations in which either parameter is constrained alone. (**b**) For the majority of duty cycle ranges, the median chi-squared value is highest for the population with both parameters constrained. (**c–d**) The Spearman's ρ values are similar at all spike numbers and duty cycle ranges for the three populations. For the g_{CaT}/g_{CaS} conductance pair, the population with high phase maintenance exhibits stronger correlations than the populations in which either duty cycle or spike number is constrained alone

noted an association between g_{CaS}/g_{KCa} correlations and general bursting activity in model neurons.

Figure 4 illustrates areas in g_{Na}/g_{CaT} conductance space that have both small (dark blue) and large (dark red) phase differences between bursters. Other conductance pairs in the single-burster study, such as g_A/g_{CaS} and g_{CaS}/g_{KCa}, had regions of bursters with low phase differences that transitioned sharply to regions of non-bursters. This suggests that g_{Na}/g_{CaT} co-regulation may exert a finer control over the intra-burst properties of the model neuron than other conductance pairs. The g_A/g_{CaS} and g_{CaS}/g_{KCa} pairs appear to be more involved in controlling overall activity type, perhaps because the g_{CaS} conductance reacts to changes in calcium on a slower time scale than the g_{CaT} conductance (Liu et al. 1998). The time constants of the various conductances, which determine the immediacy of activity-dependent conductance changes, could explain which conductances control which aspects of the model neuron's output; g_{Na} and g_{CaT} operate with fast time constants, which may enable their interplay to finely tune the spike times within bursts.

In the current body of literature, few studies have demonstrated that any calcium conductances are correlated with other conductances to regulate neuronal activity. A previous modeling study demonstrated that the g_A/g_{CaS} conductance pair resulted in tight regulation of crustacean cardiac motor neuron activity (Ball et al. 2010). This particular pair of conductances, along with the g_{CaS}/g_{KCa} pair, is also strongly correlated in several types of STG model neuron activity (Hudson and Prinz 2010), including general bursting activity. In our population study, the correlation between g_{CaS} and g_{KCa} was notably stronger in the model neuron populations with high phase maintenance than in those with low phase maintenance. While calcium currents have proven difficult to measure experimentally, the evidence from computational studies suggests that they may be involved in maintaining certain aspects of neuronal activity, including spike phase of bursting neurons.

The correlations we found in the population study apply only to bursters with periods, duty cycles, and numbers of spikes per burst within the examined ranges. Therefore, it is possible that other conductance correlations exist for bursting neurons that did not meet our criteria for analysis in this study, such as the nonlinear, concave g_{Na}/g_{Kd} correlation found in model neurons classified as bursters with only one spike per burst (Golowasch et al. 2002).

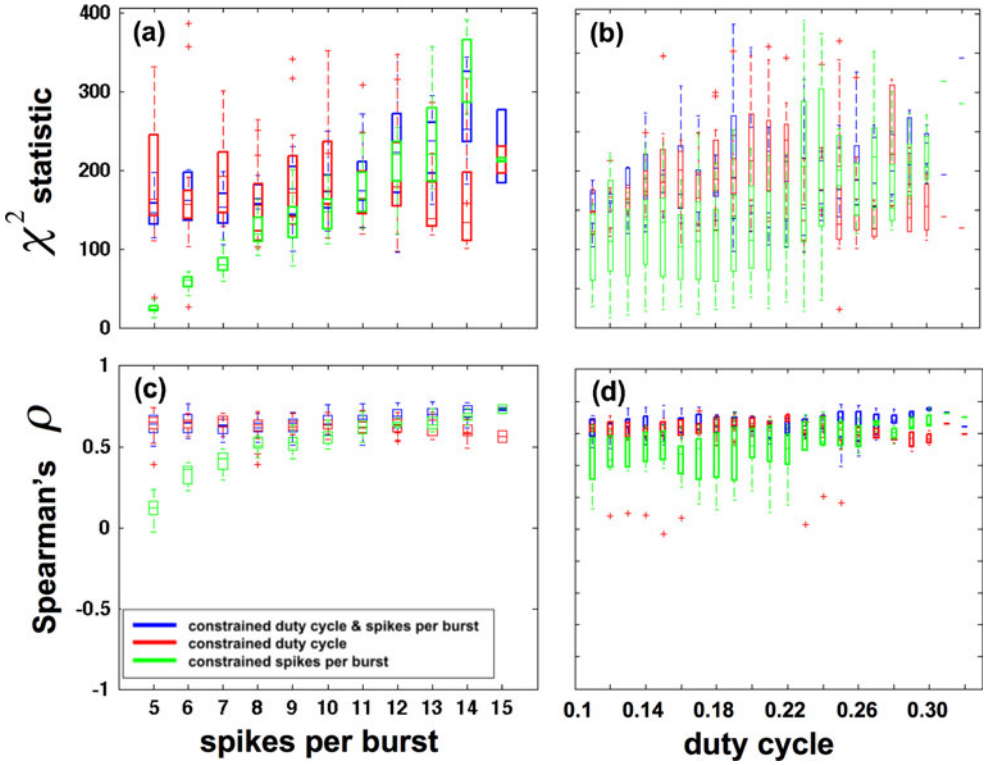

Fig. 11 Chi-squared and Spearman's ρ values for the g_{CaS}/g_{KCa} conductance pair for the three populations, plotted by number of spikes per burst and duty cycle. The middle of the boxes indicates the median values for the statistic, and the ends of the boxes indicate the lower and upper quartiles. (**a**) As the number of spikes per burst is increased, stronger correlations are seen specifically for the population of bursters with only spikes per burst constrained. Average values for the chi-squared statistic are similar for all three population types. (**b**) Stronger correlations are seen as the duty cycle is increased, but average chi-squared values are again similar between all three populations. (**c–d**) Spearman's ρ values are similar between all three population types for a range of values for duty cycle and spikes per burst

So far all conductance correlations that have been experimentally found to preserve neuronal activity in stomatogastric neurons have been positive. However, negative correlations have been seen to maintain bursting activity in large model neuron databases, including a strong negative correlation between g_A and g_{KCa} (Hudson and Prinz 2010). The present study similarly found a negative g_A/g_{KCa} correlation to be stronger in populations with highly maintained spike phases than those exhibiting a lack of phase maintenance. Hudson and Prinz also showed that a negative g_{Na}/g_{Kd} correlation preserves activity type in model neurons (2010); we saw regions of both positive and negative correlations for this conductance pair in our single-burster study (Fig. 4). From a biological perspective, we expect a positive correlation between g_{Na} and g_{Kd} to support spike phase maintenance; because g_{Na} controls a depolarizing (inward) current and g_{Kd} controls a repolarizing (outward) current, it would seem that increasing (or decreasing) one conductance would require a compensatory increase (or decrease) in the other conductance to preserve neuronal activity. For similar reasons, one might have expected g_{Na} and g_{CaT} to be inversely rather than positively correlated. We currently do not know how a positive correlation between two depolarizing currents might be useful to the neuron. Overall, the negative correlations found in the present study were fewer in number and generally weaker than the positive correlations. Indeed, the only two conductance correlations that appeared in both the single-burster and population-based studies were positive.

Modifying conductances in the biological neuron involves several layers of cellular machinery; it thus may not occur quickly enough to explain the instantaneous spike phase maintenance that is seen over time in a single neuron (Fig. 3). However, the spike phase also is maintained across different animals, despite large differences in the average burst period (Bucher et al. 2005). Thus, pairwise covariation of conductances may, at the least, provide a plausible explanation for maintenance in spike phase across animals. Possible mechanisms for this conductance covariation include ion channel co-localization on the cell membrane or translation from mRNA strands with correlated copy numbers (Schulz et al. 2007). Alternatively, the ability of pyloric neurons to maintain spike phase over time may be "built into" the electrical activity of the circuit through

adjustments to synaptic strength (Bucher et al. 2005). As with conductance-based mechanisms, a method for maintaining spike phase that relies on the electrical organization of the network is most likely not trivial and would require further investigation.

Both theoretical and experimental studies have shown that a variety of conductance relationship types can preserve neuronal activity. Linearly co-varying a potassium and a calcium conductance preserved tonic activity in both the ventricular dilator (VD) neuron of the STG and in a conductance-based model neuron (Goldman et al. 2001). Modeling studies have also demonstrated that nonlinear conductance relationships may preserve one-spike burster activity (Golowasch et al. 2002). Our single-burster modeling study, involving pairwise conductance co-variation, demonstrated phase-preserving relationships that were both linear (such as g_{CaT}/g_{Kd}) and non-linear (such as g_{Kd}/g_{leak}), and it is possible that the neuron employs both types of relationships to preserve its activity. Additionally, previous studies have revealed three- and four-way linear correlations between mRNA levels in specific STG cell types (Schulz et al. 2007). A more thorough analysis of the model neuron database may also reveal conductance relationships residing in higher dimensions for model neuron populations with specific activity constraints.

A clear future aim is to verify through experiment whether the mechanisms for phase maintenance explored in the present study are being employed by real neurons. Previous experiments have used mRNA levels to quantify channel expression, but a linear relationship between mRNA abundance and conductance value has only been found for one conductance pair: g_A and g_{KCa} (Schulz et al. 2006; Baro et al. 1997). Since mRNA injection may not reliably control the values of all conductances examined here, such an approach might not be useful as experimental verification of our results. However, multiple membrane conductances can be simulated in real time using the dynamic clamp technique. One potential future direction is to utilize dynamic clamp to modulate pairs of membrane conductances in a biological neuron while monitoring intra-burst activity to determine whether phase maintenance can be achieved via the mechanisms explored here.

Notably, the results presented above examined only spontaneous activity and do not examine the effects of synaptic input on the relationship between conductance correlations and phase maintenance. If the model neuron here were receiving regular inhibitory synaptic input, as in a network model, its steady-state activity may be altered (Prinz et al. 2003a). We have seen in the present study that altering neuronal activity may result in different patterns of conductance co-regulation (Fig. 9); the specific conductance correlations that preserve intra-burst activity may be altered by the addition of synaptic input. As an example, the present study saw no pairwise conductance correlations involving g_H. Co-regulation of the g_A/g_H pair has experimentally been shown to preserve neuronal activity, including number of spikes per burst (MacLean et al. 2005; Khorkova and Golowasch 2007). Our model may be operating in a voltage regime that does not engage the hyperpolarization-activated current, so that the value of g_H plays little role in its activity. If we were to perform a similar analysis on a model neuron receiving extra inhibitory synaptic input from other neurons, the g_H conductance might play a greater role in controlling neuronal output.

It has been hypothesized that the presence of conductance correlations has certain benefits. The fact that there are many combinations of conductances that allow the neuron to arrive at the same activity type aids in the robustness of that activity. These correlations may provide protection against drastic and potentially harmful changes to neural activity as a result of a relatively small change in one or more ionic currents.

Acknowledgements We thank Amber Hudson for informative discussions and valuable comments on the manuscript. We also thank the reviewers of the manuscript for their constructive criticism. This work was supported by grants from the National Institute of Health/National Institute of Neurological Disorders and Stroke (1F31NS071834-01 to SA and R01 NS054911 to AP), two National Science Foundation IGERT awards (to SA and WS), and a National Science Foundation Graduate Research Fellowship (to WS).

Conflicts of interest The authors declare that no conflicts of interest exist.

References

Achard, P., & De Schutter, E. (2006). Complex parameter landscape for a complex neuron model. *PLoS Computational Biology, 2*(7), e94. doi:10.1371/journal.pcbi.0020094.

Ball, J. M., Franklin, C. C., Tobin, A. E., Schulz, D. J., & Nair, S. S. (2010). Coregulation of ion channel conductances preserves output in a computational model of a crustacean cardiac motor neuron. *Journal of Neuroscience, 30*(25), 8637–8649.

Baro, D. J., Levini, R. M., Kim, M. T., Willms, A. R., Lanning, C. C., Rodriguez, H. E., et al. (1997). Quantitative single-cell-reverse transcription-PCR demonstrates that A-current magnitude varies as a linear function of shal gene expression in identified stomatogastric neurons. *Journal of Neuroscience, 17*(17), 6597–6610.

Brochini, L., Carelli, P. V., & Pinto, R. D. (2011). Single synapse information coding in intraburst spike patterns of central pattern generator motor neurons. *Journal of Neuroscience, 31*(34), 12297–12306.

Bucher, D., Prinz, A. A., & Marder, E. (2005). Animal-to-animal variability in motor pattern production in adults and during growth. *Journal of Neuroscience, 25*(7), 1611–1619.

Dayan, P., & Abbott, L. F. (2001). *Theoretical neuroscience*. Cambridge: MIT Press.

Goldman, M. S., Golowasch, J., Marder, E., & Abbott, L. F. (2001). Global structure, robustness, and modulation of neuronal models. *Journal of Neuroscience, 21*(14), 5229–5238.

Golowasch, J., Goldman, M. S., Abbott, L. F., & Marder, E. (2002). Failure of averaging in the construction of a conductance-based neuron model. *Journal of Neurophysiology, 87*(2), 1129–1131.

Graubard, K. (1978). Synaptic transmission without action potentials: input–output properties of a nonspiking presynaptic neuron. *Journal of Neurophysiology, 41*(4), 1014–1025.

Hooper, S. L. (1997a). Phase maintenance in the pyloric pattern of the lobster (Panulirus interruptus) stomatogastric ganglion. *Journal of Computational Neuroscience, 4*(3), 191–205.

Hooper, S. L. (1997b). The pyloric pattern of the lobster (Panulirus interruptus) stomatogastric ganglion comprises two phase-maintaining subsets. *Journal of Computational Neuroscience, 4* (3), 207–219.

Hooper, S. L., & Weaver, A. L. (2000). Motor neuron activity is often insufficient to predict motor response. *Current Opinion in Neurobiology, 10*(6), 676–682.

Hudson, A. E., & Prinz, A. A. (2010). Conductance ratios and cellular identity. *PLoS Computational Biology, 6*(7), e1000838. doi:10.1371/journal.pcbi.1000838.

Huguenard, J. R., & McCormick, D. A. (1992). Simulation of the currents involved in rhythmic oscillations in thalamic relay neurons. *Journal of Neurophysiology, 68*(4), 1373–1383.

Khorkova, O., & Golowasch, J. (2007). Neuromodulators, not activity, control coordinated expression of ionic currents. *Journal of Neuroscience, 27*(32), 8709–8718.

Lago-Fernandez, L. F. (2007). Spike alignment in bursting neurons. *Neurocomputing, 70*, 1788–1791.

Latorre, R., Rodriguez, F. B., & Varona, P. (2006). Neural signatures: multiple coding in spiking-bursting cells. *Biological Cybernetics, 95*(2), 169–183.

LeMasson, G., Marder, E., & Abbott, L. F. (1993). Activity-dependent regulation of conductances in model neurons. *Science, 259*(5103), 1915–1917.

Levitan, I. B. (1988). Modulation of ion channels in neurons and other cells. *Annual Review of Neuroscience, 11*, 119–136.

Liu, Z., Golowasch, J., Marder, E., & Abbott, L. F. (1998). A model neuron with activity-dependent conductances regulated by multiple calcium sensors. *Journal of Neuroscience, 18*(7), 2309–2320.

MacLean, J. N., Zhang, Y., Johnson, B. R., & Harris-Warrick, R. M. (2003). Activity-independent homeostasis in rhythmically active neurons. *Neuron, 37*(1), 109–120.

MacLean, J. N., Zhang, Y., Goeritz, M. L., Casey, R., Oliva, R., Guckenheimer, J., et al. (2005). Activity-independent coregulation of IA and Ih in rhythmically active neurons. *Journal of Neurophysiology, 94*(5), 3601–3617.

Marder, E. (1997). Computational dynamics in rhythmic neural circuits. *The Neuroscientist, 3*, 295–302.

Marder, E., & Bucher, D. (2007). Understanding circuit dynamics using the stomatogastric nervous system of lobsters and crabs. *Annual Review of Physiology, 69*, 291–316.

Morris, L. G., & Hooper, S. L. (1997). Muscle response to changing neuronal input in the lobster (Panulirus interruptus) stomatogastric system: spike number- versus spike frequency-dependent domains. *Journal of Neuroscience, 17*(15), 5956–5971.

Morris, L. G., Thuma, J. B., & Hooper, S. L. (2000). Muscles express motor patterns of non-innervating neural networks by filtering broad-band input. *Nature Neuroscience, 3*(3), 245–250.

Prinz, A. A., Billimoria, C. P., & Marder, E. (2003a). Alternative to hand-tuning conductance-based models: construction and analysis of databases of model neurons. *Journal of Neurophysiology, 90* (6), 3998–4015.

Prinz, A. A., Thirumalai, V., & Marder, E. (2003b). The functional consequences of changes in the strength and duration of synaptic inputs to oscillatory neurons. *Journal of Neuroscience, 23*(3), 943–954.

Prinz, A. A., Bucher, D., & Marder, E. (2004). Similar network activity from disparate circuit parameters. *Nature Neuroscience, 7*(12), 1345–1352.

Raper, J. A. (1979). Nonimpulse-mediated synaptic transmission during the generation of a cyclic motor program. *Science, 205*(4403), 304–306.

Schulz, D. J., Goaillard, J. M., & Marder, E. (2006). Variable channel expression in identified single and electrically coupled neurons in different animals. *Nature Neuroscience, 9*(3), 356–362.

Schulz, D. J., Goaillard, J. M., & Marder, E. E. (2007). Quantitative expression profiling of identified neurons reveals cell-specific constraints on highly variable levels of gene expression. *Proceedings of the National Academy of Sciences of the United States of America, 104*(32), 13187–13191.

Selverston, A. I. (2010). Invertebrate central pattern generator circuits. *Philosophical Transactions of the Royal Society of London. Series B, Biological Sciences, 365*(1551), 2329–2345.

Selverston, A. I., & Moulins, M. (1985). Oscillatory neural networks. *Annual Review of Physiology, 47*, 29–48.

Swensen, A. M., & Bean, B. P. (2003). Ionic mechanisms of burst firing in dissociated Purkinje neurons. *Journal of Neuroscience, 23*(29), 9650–9663.

Swensen, A. M., & Bean, B. P. (2005). Robustness of burst firing in dissociated purkinje neurons with acute or long-term reductions in sodium conductance. *Journal of Neuroscience, 25*(14), 3509–3520.

Szucs, A., Pinto, R. D., Rabinovich, M. I., Abarbanel, H. D., & Selverston, A. I. (2003). Synaptic modulation of the interspike interval signatures of bursting pyloric neurons. *Journal of Neurophysiology, 89*(3), 1363–1377.

Tobin, A. E., Cruz-Bermúdez, N. D., Marder, E., & Schulz, D. J. (2009). Correlations in ion channel mRNA in rhythmically active neurons. *PLoS One, 4*(8), e6742. doi:10.1371/journal.pone.0006742.

Turrigiano, G., LeMasson, G., & Marder, E. (1995). Selective regulation of current densities underlies spontaneous changes in the activity of cultured neurons. *Journal of Neuroscience, 15*(5 Pt 1), 3640–3652.